Journal of Ceramic Processing Research. Vol. 12, No. 1, pp. 106~109 (2011)

J O U R N A L O F
Ceramic Processing Research

Catalyst-free growth of ZnO nanowires on Si (100) substrates by thermal evaporation

Tran Van Khai, Sin Young Bang, Dong Keun Oh, Bong Geun Choi and Kwang Bo Shim*

Division of Advanced Materials Science Engineering, Hanyang University, 17 Haengdang-dong, Seongdong-Gu, Seoul 133-791, South Korea

Vertically well-aligned ZnO nanowires with a high density were successfully grown on Si (100) substrates without a catalyst by conventional thermal evaporation. The grown ZnO nanowires are relatively uniform in diameter of about 180 nm and length of about 4 μm. They exhibit the morphological features of faceted planes at the tips of hexagonal columns and are preferentially oriented along the [001] direction. The optimum growth condition was obtained from the experimental result that the degree of vertical alignment of the ZnO nanowires depends sensitively on the distance between the substrate and the Zn source. The PL characteristics of the grown ZnO nanowires reveal a strong and sharp UV emission at 380 nm and a broad green emission in the region of 500 nm, indicating excellent optical properties.

Key words: ZnO nanowires, thermal evaporation, photoluminescence, nanostructure.

Introduction

In recent years, there has been increasing interest in economical synthesis methods for quasi-one-dimensional (1D) nanostructures such as nanowires, nanorods, nanobelts and nanotubes due to their unique physical properties and potential applications in electronics, optics, photonics and sensing devices [1]. The nano-scaled ZnO structure is one of most promising cases since ZnO possesses not only a wide band gap of 3.37 eV with a large exciton binding energy of 60 meV at room temperature but also high mechanical and thermal stabilities.

Among many synthesizing methods of ZnO nanostructures [2-6], thermal evaporation [7] is very attractive because of the ease control of processing and it is a relatively low cost synthesizing system. Most studies on the thermal evaporation of ZnO nanostructure have used catalysts such as Au [8-11], Cu [12], Sn [13] or other additives such as Ga [14] and NiO [15] in order to assist and control the growth process. However, the catalysts or additives can easily remain in the final ZnO structure, resulting in unfavorable properties. Therefore, the remaining catalyst or additives should be completely removed from the grown ZnO nanowires. Additionally, a silicon (Si) substrate has an advantage in the semiconductor integrated processing techniques since Si is relatively inexpensive and compatible with electronic devices, compared with the conventionally used sapphire substrate. However, it is not easy to directly grow well-aligned ZnO nanowires on a Si substrate because the large differences in the lattice constants and the thermal expansion characteristics between the ZnO nanowires and the Si substrates would introduce a rather large residual strain [16, 17]. Until now, only a few research studies on the catalysis-free growth of ZnO nanowires on Si substrates have been reported [18-20] even though this process seems to be very preferable from an industrial viewpoint. This study is aimed at establishing the optimum growth conditions for vertically aligned ZnO nanowire arrays on Si (100) substrates without a catalyst.

*Corresponding author:
Tel : +39-011-564-4674
Fax: +39-011-564-4699
E-mail: kbshim@hanyang.ac.kr

Experimental Details

A horizontal tube furnace was used for the thermal evaporating deposition and was composed of the two heating zones of 300 mm. Si (100) wafers (1×1 cm^2) and metallic Zn powders (75 μm, 99.99%, Sigma-Aldrich, USA) were used as substrates and source material, respectively. Initially, the substrate was etched with an H_3PO_4 (80%) solution for one minute to remove the native oxide layer on the surface and then cleaned with a sequence of acetone, methanol, de-ionized water and finally dried by air [21]. A schematic diagram of the experimental set-up is shown in Fig. 1. In order to investigate the effect of the distance (l) between the Zn source and the substrate on the morphological features of the grown ZnO nanowires, the substrates were loaded to different positions (A, B and C) with the other growth conditions fixed. The Zn source was thermally vaporized to synthesize ZnO nanowires in Ar (99.999%) flowing atmospheres of 350 standard cubic centimetre mass (sccm) for 90 minutes at 620 °C.

The grown ZnO nanowires were studied by X-ray diffraction (XRD, Rigaku, Japan) for the crystalline phase analysis and were characterized by a scanning electron microscope (SEM, JSM 5900 LV, JEOL, Japan) and a transmission electron microscope (TEM, JEOL JEM-4010,

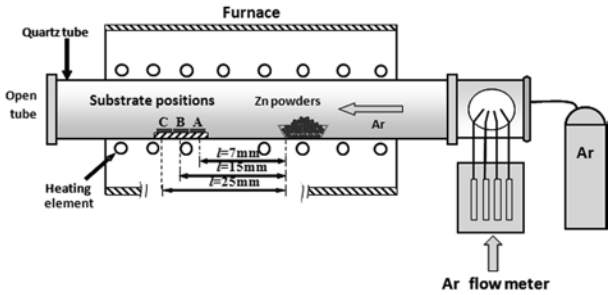

Fig. 1. A schematic diagram of the experimental apparatus for the growth of ZnO nanowires. The substrate positions (A, B, C) are distant from Zn source, corresponding to the distances (l): A = 7 mm, B = 15 mm and C = 25 mm.

400 kv, Japan) for the morphological, chemical and structural features. The photoluminescence (PL) measurements were performed using the 325 nm line of a He-Cd laser as the excitation source with a 350 nm filter.

Results and Discussion

Fig. 2 shows the alignment feature of ZnO nanowires as a function of the Si substrate position. The degree of the alignment of ZnO nanowires increases by shortening the distance (*l*). The ZnO nanowires were randomly grown at position 'C' and slightly deviated from the exact vertical direction at position 'B'. However, at position 'A', they are vertically well-aligned with the substrate and their diameter and length also increase, exhibiting that almost the entire surface of the substrate is covered with the ZnO nanowires, even on the sides of the substrate. This can be explained in that the temperature of the substrate region is lower than that of the Zn source due to the temperature gradient and the substrate temperature increases by shortening the distance between the Zn source and substrate. Therefore, it can be suggested that the degree of vertical alignment of the grown ZnO nanowires depends on the local substrate temperature [15, 22]. The XRD analysis of the grown ZnO nanowires also reveals that the intensity and sharpness of the (002) peaks increase dramatically by shortening the distance (*l*), indicating that the ZnO nanowires grown at the position 'A' are preferably oriented along the direction perpendicular to the Si (100) substrates and possess excellent crystallinity (Fig. 3). It is seen that all diffraction peaks are well matched with the wurtzite structure of single-crystalline ZnO.

Fig. 4(a-b) show SEM images of the ZnO nanowires grown at position 'A'. All ZnO nanowires are seen to be individually separated and have uniform diameters as shown in Fig. 4(a). A magnified image in the upper right corner shows clearly that the top of the ZnO nanowires are flat with a hexagonal shape. There is no hemispherical shape found at the top end of the nanowires, which is usually found in catalytically grown ZnO nanowires [23]. This result indicates that the nanowires have a clean surface and were synthesized with a high quality. Fig. 4(b) shows

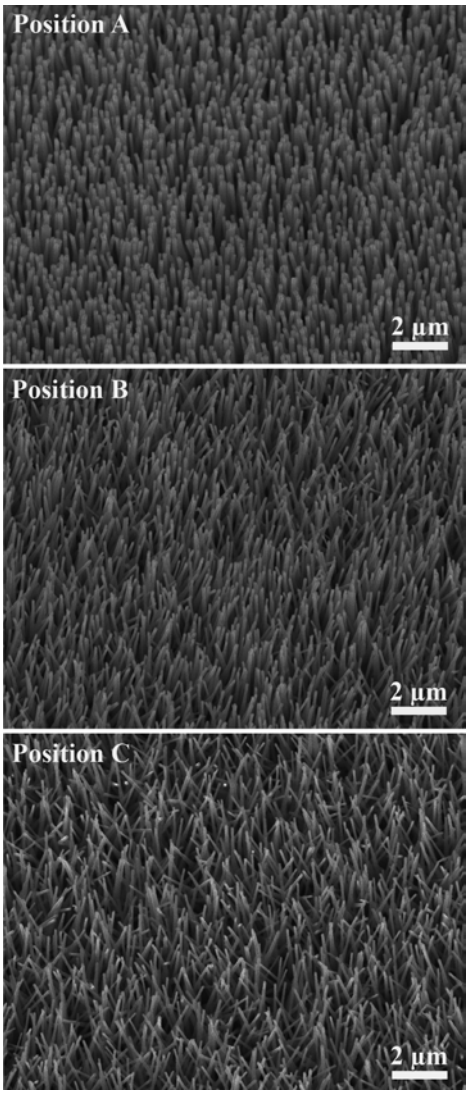

Fig. 2. SEM images of the grown ZnO nanowires as a function of the substrate position.

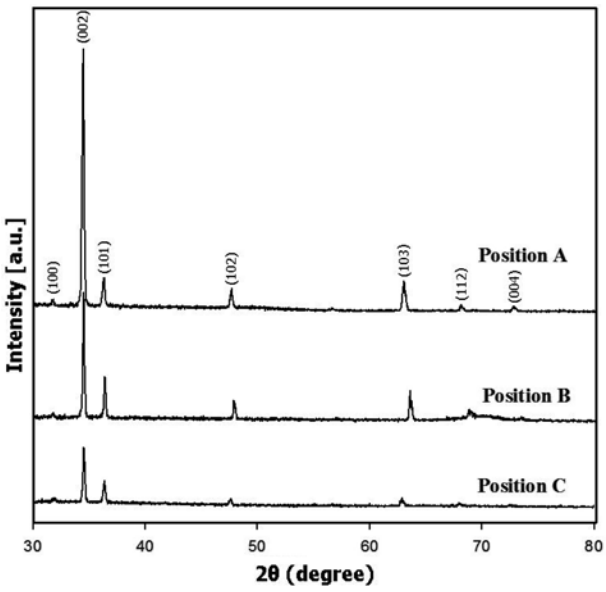

Fig. 3. XRD patterns of the grown ZnO nanowires as a function of the substrate position.

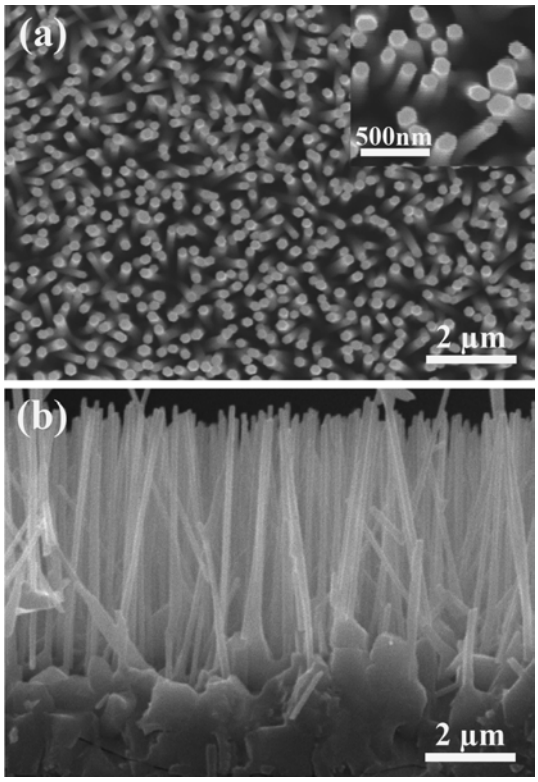

Fig. 4. SEM images of the ZnO nanowires grown at position 'A': (a) Top-view and (b) Side-view.

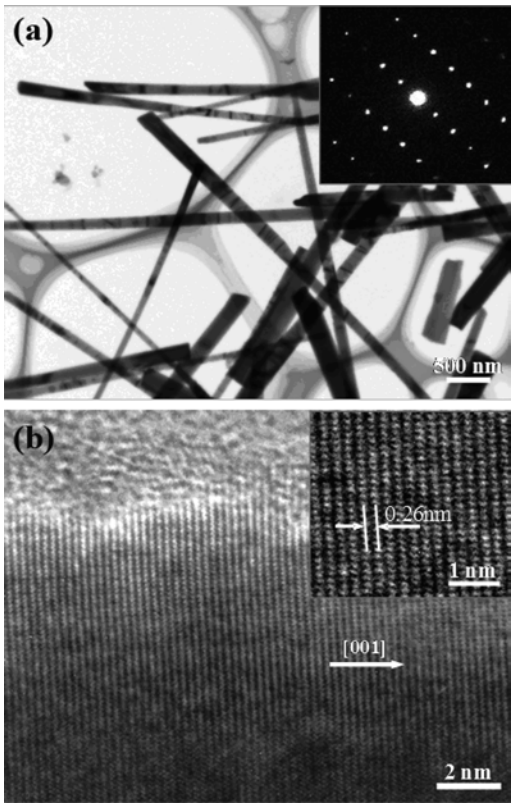

Fig. 5. TEM images of the ZnO nanowires grown at position 'A': (a) conventional TEM; the inset shows the corresponding SAED pattern and (b) HR-TEM; the inset is a high-magnification TEM image showing that the measured lattice spacing indicates the nanowire growth is along the [001] direction.

the ZnO nanowires grown in a vertical direction with a length of about 4 μm, and that the nanowires have smooth surfaces.

Since no metal catalyst or buffer layer was used to synthesize the aligned ZnO nanwire arrays, it can be suggested that the conventional vapor liquid solid (VL) model did not operate to grow these ZnO nanowire arrays. As for the mechanism of the nanowire growth, previous reports [24-26] have suggested that nucleation at the initial stage plays a crucial role in both the vertical and in-plane alignments of the ZnO nanostructure arrays. At the initial nucleation stage, the vapor Zn is oxidized quickly and then condensed on the substrate to form ZnO nuclei. Each ZnO nuclei might consist of a single crystal ZnO, which is similar to the epitaxial growth of single crystalline ZnO films on Si substrates [27]. Nanowires are then assembled on the top of the nuclei particles and grow upwards continually.

Detailed structural features of the as-grown ZnO nanowires are shown in Fig. 5(a-b). Fig. 5(a) shows that the ZnO nanowires obtained have a relatively straight shape and uniform diameters of about 180 nm along their lengths. The selected-area electron diffraction (SAED) pattern confirms that the ZnO nanowire has a single-crystal hexagonal structure. The HR-TEM image of a single ZnO nanowire of Fig. 5(b) shows that the ZnO nanowire contains no defects such as dislocations and stacking faults, indicating that it has a clean surface structure of an excellent quality. The inset in Fig. 5(b) is the lattice-resolved HR-TEM image of a segment of a single ZnO nanowire. It is seen clearly that the ZnO crystal lattice is well-oriented with no observable structural defects over the whole region. This result indicates that the ZnO nanowires obtained are structurally homogeneous and defect-free. The lattice spacing of the ZnO nanowire is about 0.26 nm, corresponding to the distance between two (002) crystal planes, confirming that the ZnO nanowires are preferentially grown along the [001] direction.

The optical properties of the ZnO nanowires obtained are presented in Fig. 6. A strong and sharp UV near-band-emission is observed at 380 nm and a suppressed and broad green emission near 500 nm. Similar results are found in other papers [18, 28-30]. The UV emission is clearly understood as a near-band-edge (NBE) emission of the wide band gap of ZnO, which originates from the recombination of free-excitons through an exiciton-exiciton collision process [4, 14]. On the other hand, a green-yellow band emission is usually attributed to a deep level emission caused by the impurities or the structural defects such as Zn interstials, oxygen vacancies and sub-surface lattices of the ZnO structure [31] and/or to the radial recombination of a photo-generated hole with singly ionized charged state of the defects in the ZnO [32]. In addition, it has been suggested that the intensity of the green band is size-dependent such that the intensity increases as the wire diameter decreases, indicating the existence of oxygen vacancies or defects in the surfaces of the nanowires [33, 34].

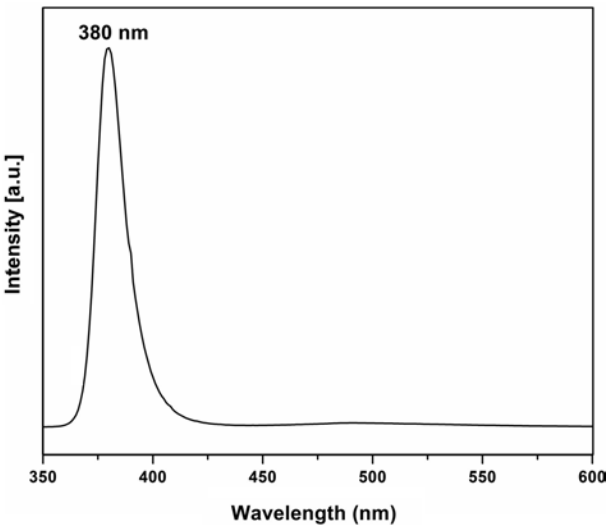

Fig. 6. Room-temperature PL spectrum of the ZnO nanowires grown at position 'A'.

Therefore, the clear appearance of strong and sharp UV emission of the grown ZnO nanowires confirms their high crystal quality and the weak broad green-yellow emission indicates the possibility of the presence of a few structural defects in the nanowires.

Conclusions

Vertically well-aligned ZnO nanowires were successfully grown on Si substrates without a catalyst or additives by a simple thermal evaporation method. The grown ZnO nanowires have uniform sizes in diameter and in length. It was found that the distance between the Zn source and substrate is an important factor for the vertical alignment of the ZnO nanowires along the direction normal to the Si (100) substrate surface. The grown ZnO nanowires possess good crystallinity and exhibit excellent optical properties. It may be concluded that the successful catalyst-free growth of ZnO nanowires may have opened up opportunities for fabricating one dimensional nanowires of a high quality, a vertical alignment and for large-scale production.

References

1. Y. Xia, P. Yang, Y. Sun, Y. Wu, B. Mayers, B. Gates, Y. Yin, F. Kim and H. Yan, Adv. Mater 15 (2003) 353-389.
2. W.I. Park, D.H. Kim, S.W. Jung and G.C. Yi, Appl. Phys. Lett. 80 (2002) 4232-4234.
3. B.P. Zhang, N.T. Binh, Y. Segawa, K. Wakatsuki and N. Usami, Appl. Phys. Lett. 83 (2003) 1635-1637.
4. Y.C. Kong, D.P. Yu, B. Zhang, W. Fang and S.Q Feng, Appl. Phys. Lett. 78 (2001) 407-409.
5. Y. Sun, G.M. Fuge and M.N.R. Ashfold, Chem. Phys. Lett. 396 (2004) 21-26.
6. M.H. Huang, Y. Wu, H. Feick, N. Tran, E. Weber and P. Yang, Adv. Mater. 13 (2001) 113-116.
7. C. Li, G. Fang, S. Xu, D.S. Zhao and X.Z. Zhao, Nanotechnology 17 (2006) 5367-5372.
8. M.H. Huang, S. Mao, H. Feick, H.Yan, Y. Wu, H. Kind, E. Weber, R. Russo and P.Yang, Science 292 (2001) 1897-1899.
9. H.J. Fan, B. Fuhrmann, R. Scholz, F. Syrowatka, A. Dadgar, A. Krost and M. Zacharias, J. Cryst. Growth 287 (2006) 34-38.
10. H.J. Fan, F. Fleisher, W. Lee, K. Nielsch, R. Scholz, M. Zacharias, U. Gösele, A. Dadgar and A. Krost, Superlattice Microst. 36 (2004) 95-105.
11. H.K. Park, M.H. Oh, S.W. Kim, G.H. Kim, D.H. Youn, S. Lee, S.H. Kim, K.C. Kim and S.L. Maeng, ETRI J 28 (2006) 787-789.
12. S.Y. Li, C.Y. Lee and T.Y. Tseng, J. Cryst. Growth 247 (2003) 357-362.
13. P.X. Gao, Y. Dinh and Z.L. Wang, Nano Lett. 9 (2004) 1315-1320.
14. Y.K. Tseng, C.J. Huang, H.M. Cheng, I.N. Lin, K.S. Liu and I.C. Chen, Adv. Funct. Mater. 13 (2003) 811-814.
15. S.C. Lyu, Y. Zhang, C.J. Lee, H. Ruh and H.J. Lee, Chem. Mater. 15 (2003) 3294-3299.
16. Y. Zhang, H. Jia and D.Yu, J. Phys. D: Appl. Phys. 37 (2004) 413-415.
17. H.C. Hsu, C.S. Cheng, C.C. Chang, S. Yang, C.S. Chang and W.F. Hsieh, Nanotechnology 16 (2005) 297-301.
18. C. Geng, Y. Jiang, Y. Yao, X. Meng, J.A. Zapien, C.S. Lee, Y. Lifshitz and S.T. Lee, Adv. Funct. Mater .14 (2004) 589-594.
19. J.S. Jeong, J.Y. Lee, J.H. Cho, C.J. Lee, S.J. An, G.C. Yi and R. Gronsky, Nanotechnology 16 (2005) 2455-2461.
20. H. Ham, G.Shen, J.H. Cho, T.J. Lee, S.H. Seo and C.J. Lee, Chem. Phys. Lett. 404 (2005) 69-73.
21. S.Y. Bang, W.S. Kim, J.H. Chung, B.G. Choi and K.B. Shim, J. K. Cryst. Growth and Cryst. Tech. 2 (2008) 81-86.
22. A. Umar, S.H. Kim, E.K. Suh and Y.B. Hahn, J. Cryst. Growth 306 (2007) 52-61.
23. H.K. Park, M.H. Oh, S.W. Kim, G.H. Kim, D.H. Youn, S. Lee, S.H. Kim, K.C. Kim and S.L. Meang, ETRI J 28:(2006) 787-789.
24. G.W. Cong, H.Y. Wei, P.F. Zhang, W.Q. Peng, J.J. Wu, X.L. Lui, C.M. Jiao, W.G. Hu, Q.S. Zhu and Z.G. Wang Appl. Phys. Lett. 87 (2005) 231-903.
25. H.P. Tang, L.P. Zhu, Z.H. Ye, H.P. He, Y. Zhang, M.G. Zhi, F. Yang, Z.X. Yang and B. Zhao, Mater. Lett. 61 (2007) 1170-1173.
26. M. Wang, C.H. Ye, Y. Zhang, G.M. Hua, H.X. Wang, M.G. Kong and L.D. Zhang, J. Cryst. Growth 291(2006) 334-339.
27. H. Rumpf, in "The Strength of Granules and Agglomerates: International Symposium on Agglomeration,"(Interscience, London, 1962) p. 379-418.
28. J.Y. Kim, H.W. Shim, E.K. Sun, T.Y. Kim, S.H. Lee, Y.H. Mo and K.S. Nahm, J. Korean Phys. Soc. 44 (2004) 137-139.
29. A. Umar, H.W. Ra, J.P. Jeong, E.K. Suh and Y.B. Hahn, Korean J. Chem. Eng. 23 (2006) 499-504.
30. W.Y. Song, J.H. Yang, D.V. Dinh, T.I. Shin, S.M. Kang, S.W. Kim and D.H. Yoon J. Phys. Chem. Solids 69 (2008) 1486-1490.
31. W.I. Park, G.C. Yi, M. Kim and S.J. Pennycook, Adv. Mater. 14 (2002) 1841-1843.
32. K. Vanheusden, W.L. Warren, C.H. Seager, D.K. Tallant, J.A. Voigt and B.E. Gnade, J. Appl. Phys. 79 (1996) 7983-7985.
33. B.J. Jin, S.H. Bae, S.Y. Lee and S. Im, Mater. Sci. Eng. B 71 (2000) 301-305.
34. P. Yang, H. Yan, S. Mao, R. Russo, J. Johnson, R. Saykally, N. Morris, J. Pham, R. He and H.J. Choi, Adv. Funct. Mater. 12 (2002) 323-331.